Performance of Parameterization Algorithms for Resident Space Object (RSO) Attitude Estimates

Ryan Clark

Sidharth Dave, Jack Wawrow, Regina Lee.

York University, 4700 Keele Street, Toronto, Ontario M1J 1P3, Canada

Abstract

The lack of Space Situational Awareness (SSA) for Low Earth Orbit has been a growing concern in the space sector. The number of tracked objects is estimated to double in the next decade; therefore, better SSA methods are required to keep up with this increase. Optical detections have been demonstrated to estimate a Resident Space Object (RSO) shape, attitude and optical properties with a sufficiently accurate priory information. Different light curve inversion techniques have demonstrated feasibility from ground-based optical detections, however they have not been demonstrated on passive space-based optical sensors such as Star Trackers. This paper presents the results of a feasibility study for a novel application of estimating an RSO's shape, attitude and optical properties from space-based passive detections. The first part of the feasibility study uses a star tracker image simulator to simulate space-based RSO detections and produce light curves from RSO's in a controlled environment. The simulation uses a forward ray tracing model to recreate the image. Four different RSO shape models are used: 1U CubeSat, 3U CubeSat, Box-Wing cube satellite, and Iridium First Gen. Five different methods of parameter optimization for an RSO's shape, attitude and optical parameters are being tested: Gradient Descent, Stochastic Hill Climbing, Simulated Annealing, a Genetic Algorithm and Particle Swarm Optimization. The feasibility of this novel application will be based off the accuracy of the estimated parameters, as well as the computational efficiency of each algorithm to converge on a RSO's shape, attitude, and optical properties.

1 Introduction

The Resident Space Object (RSO) population is rapidly growing in numbers, which has become a significant concern worldwide. Today, according to NASA, more than 22,000 objects that are larger than 10-cm in diameters are in Earth orbit; many more objects that are smaller than 10-cm diameters are estimated to be in orbit. It is still not clear how many hundreds of thousands of uncatalogued debris pose threats to space assets around the world. While there are continuing collaborative efforts among various space agencies and research communities to monitor the space objects from the ground and on-orbit, a large number of uncertainties in RSO numbers, trajectories and identifies still remain. In this paper, we present a novel method to estimate RSO shape, attitude and optical properties using their light curve characteristics to enhance tracking and identification of RSOs, namely Space Situational Awareness (SSA). SSA is an important aspect of establishing space resiliency as an effective means to recognize, view, track, and forecast potential threats; much of the SSA comes from RSO's. In future missions, it is anticipated that the further study of optical imaging of RSOs will lead to the investigation of precise orbit determination, shape and attitude of the RSOs by closely examining light curves.

Light curve refers to a time series of the RSO's brightness versus time as received by a sensor. Characterization of RSO properties using a light curve is a well-known approach in both astrophysics and RSO studies. In [1], for example, the authors present a new technique to interpret the light curves of debris objects. In [2], a complex modeling technique to simulate space-based surveillance images considers photometric light curves. In Section 2 of this paper, we provide an overview of recent studies on RSO characterization using light curve. The majority of the optical detection and light curve analysis are based on ground observations; limited studies reported on space-based observations.

Ground-observations of RSO's are often managed by national space agencies. In the United States, GEODSS network provides the 'backbone' of the SSA effort. In [3], a major weakness of the GEODSS architecture is described as "*not provide[ing] world-wide coverage; the present network has a wide gap in coverage over Western Europe and a narrow gap in coverage over East Asia. As the great 40 inch refractor at the Yerkes Observatory, Williams Bay,*

Wisconsin, is still in operation after more than 115 years, there is no reason the GEODSS network cannot remain effective for many more decades."

Comparatively, the European Space Agency's (ESA) Space Surveillance and Tracking (SST) activities are undertaken by the SSA program with Space Weather and Near-Earth Object tracking. In [4], an overview of SSA trends are presented; various sensors are listed, including optical, radar, RF and laser ranging for SST. In Canada, DRDC reports several observation sites with SST capabilities; for example, [5] describes the DRDC Ottawa Space Surveillance Observatory; another example is showcased in [6] where it demonstrates ground-based observation of the light curve of a small satellite.

Although ground-observation provides the baseline of SST and there is continuing effort to advance algorithms, automation and operationalization of RSO tracking, challenges pertaining to the robustness and resilience of these systems still remain. Some disadvantages that come from ground-based observation include atmospheric scattering, temporal restrictions, possible weather interference, and viewing angle restrictions.

In comparison, space-based observations ignores atmospheric and weather effects, is not limited to nighttime observations and can view RSO's at multiple viewing angles. Currently, the largest well-known space-based SST mission is Space Based Space Surveillance by the United States DOD. Canada has already invested in building capabilities to track RSOs, such as the Sapphire and NEOSSAT missions [7]. Unfortunately, to date, there are no other currently planned on-orbit Canadian SSA missions to replace aging satellites; both Sapphire and NEOSSat have now exceeded the original mission design lifetimes. The missions described here are dedicated SST spacecrafts capable of selecting and tracking target RSOs. Disadvantages that accompany dedicated sensors are long lead times, high cost, and smaller coverage of regions of space.

We proposed an alternative to the space-based dedicated SST mission to rely on passive observation using low-resolution imagers with observation-of-opportunity for RSO tracking and identification. Star trackers have been proven feasible for RSO tracking from pervious works, such as in [8]. Fig 1 below (left) illustrates a sample FAI image where three RCM is visible.

Figure 1: FAI Image with RADARSAT Constellation Mission in FOV [9]

In the current study, we focused on light curve inversion using low-resolution images to take advantage of the observation-of-opportunities. Light curve 'inversion' refers to the process of modeling the surfaces (facets or shape) of an object from their brightness variations; in this case, reflected light. There are several commonly used techniques in light curve inversion, most of which follow the same underlying method:

- Using the shape, optical properties, and attitude to estimate the brightness of the RSO
- Comparing the brightness to the observed brightness of the object (represented by the light curve)
- Updating the shape, optical properties, and attitude estimate to reduce the error between the true and estimated brightness

In the remaining paper, we describe the overview of recent studies on RSO light curve analysis, followed by a brief review on optimization methods suitable for RSO cauterization. In Section 3, we describe the methods and algorithms we have implemented for RSO attitude estimation. We outline the results from the simulation study in Section 4, with a comparison of optimization algorithms under investigation. The last section of the paper summarizes the conclusion and suggests future tasks for further analysis of light curve.

2 Background

2.1 Light Curve Generation

In the context of the current study on RSO characterization, light curve represents temporal brightness of an object that reflects light, such as active or deactivated satellites, rocket bodies, debris and other objects in orbit. Several parameters play critical roles in the brightness of a reflected object, including the most obvious physical dimensions like size and shape, as well as the geometry and distance of the object. Additionally, the facet model and Bidirectional Reflectance Distribution Function (BRDF), relative motion (referred to as attitude) of the object and the optical surface properties all effect the brightness received from the RSO.

The most common approach in presenting RSO's characteristics as light curve is to use a simple sphere to estimate RSO optical signatures as described in [10]. Such simplification is considered a good approximation for detections as they represent the location and relative size of the RSO. This provides useful information for detections, however, does not include the needed information for RSO characterisation. For characterisation of RSO's, a more sophisticated model is required to account for the RSO's shape, attitude, and difference reflecting surfaces. Such models generally break down the 3D shape of the satellite into a combination of 2D reflecting surfaces or facets.

The facets are represented by shapes that have a well-defined Bidirectional Reflectance Distribution Function (BRDF). Various BRDF models for the facets are available with the first facets models for satellites being introduced in the late 1970's [11] [12].

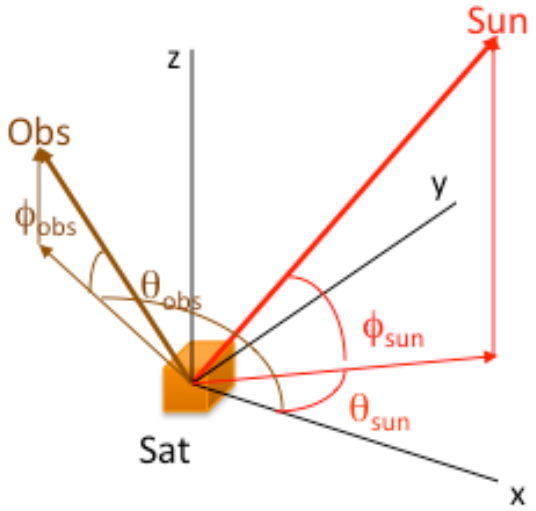

Figure 2 RSO Illumination Geometry [30]

Table 1 lists the diffuse verses specular conditions for reflection and the respective BRDF model for each facet. Figure 2 represents the viewing geometry for

Table 1. In

Table 1: Δ represents the angular size of the sun from Earth, and $\alpha(t)$ represents a function of the visible cord of the sun [11]. In this study, we used three facets (flat surface, sphere and cylinder) to represent 3D shapes with varying degrees of curvature across a facet. Diffuse reflection refers to the reflection where the angle of incidence is not the angle of reflection. Specular, or mirror like, reflection occurs when the angle of incidence is equal to the angle of reflection. Generally, specular reflections are orders of magnitude brighter than diffuse reflection.

Table 1: Facet Dependent Phase Function

Facet Type (Degrees of Curvature)	**Sphere (2)**	**Flat Surface (0)**	**Cylinder (1)**
Diffuse Phase Condition	None	ϕ_{obs} and ϕ_{sun} are the same sign	None
Diffuse Phase Equation	$\frac{2}{3\pi^2}[(\pi-\Phi)\cos(\Phi)+\sin(\Phi)]$	$\frac{1}{\pi}\sin(\phi_{obs})\sin(\phi_{sun})$	$\frac{\cos(\phi_{obs})\cos(\psi_{sun})}{4\pi}[(\pi-\theta)\cos(\theta)+\sin(\theta)]$
Specular Phase Condition	None	$\lvert\phi_{obs}-\phi_{sun}\rvert \leq \frac{\Delta}{2}$ & $\lvert\theta_{sun}-\theta_{obs}\rvert = \pi$	$\lvert\phi_{obs}-\phi_{sun}\rvert \leq \frac{\Delta}{2}$
Specular Phase Equation	$\frac{1}{4\pi^2}$	$\frac{4\cos(\Phi/2)}{\pi\Delta^2}$	$\frac{\cos(\Phi/2)\ \alpha(t)}{4\Delta}$

For the simulation study, we implemented the defined facet model [13] [14] that uses well-defined facet shapes and BRDF's as shown in

Table 1, with equation 1 and 2 to calculate the reflected brightness:

$$m_v = m_o - 2.5\log\frac{\sum \rho_i A_i F(\Phi)_i}{R^2} \quad (1)$$

$$F(\Phi)_i = B_{diff,i}F(\Phi_i)_{diff} + B_{spec,i}F(\Phi_i)_{spec} \quad (2)$$

In equation 1 and 2: m_v represents the apparent magnitude of the RSO; m_o represents the apparent magnitude of the sun; ρ_i represents the reflectivity of the i[th] facet; A_i represents the effective area of the i[th] facet; Φ_i represents the Sun, RSO facet, and Observer phase angle; R represents the RSO to Observer distance; $B_{diff,i}$ and $B_{spec,i}$ represent the Hejduk Coefficients [13].

2.2 Optimization Algorithm

There are several optimization methods that have been successfully applied to light curve inversion. In [15] and [16], various methods including the octant triangulation, convex hull algorithm were applied for asteroid light curve inversion. For RSO's, similar techniques have been implemented: Unscented Kalman Filters [17], MMEA [14], and different machine learning models [18]. In this study, we examined 5 commonly used optimization techniques: (1) Gradient Descent; (2) Stochastic Hill Climbing; (3) Simulated Annealing; (4) Genetic Algorithm; and (5) Particle Swarm Optimisation. These are all well-known, widely used techniques in non-linear problems, where both the problem and the boundary conditions are established with varying degrees of certainty. In this section, each method is briefly summarised for comparison; some general terms are defined for the context of this paper before each method is summarized. The objective function that the parameterisation algorithms are solving is the residual between the real and simulated light curve, with the goal to find a global minimum for this value.

Gradient Descent is the most common, first-order iterative optimization algorithm. Recently, this simple algorithm has been successfully used in machine learning to update parameters in linear regression. It has the advantage of being easily coded and computationally efficient to run compared to other parameterisation algorithms. In [19], Ruder explains the fundamentals of this popular algorithm as "*a way to minimize an objective function J(θ) parameterized by a model's parameters* $\theta \in R$ *d by updating the parameters in the opposite direction of the gradient of the objective function* $\nabla\vartheta J(\vartheta)$ *with respect to the parameters.*"

Stochastic Hill Climbing (SHC) is a global optimization algorithm with two stages: global search and local search. SHC behaves much like Hill Climbing algorithms; the difference being that a random positive step is taken instead of the best step. SHC starts with the global search phase, having the goal of covering as much ground as possible in the design space so that global optimum does not get missed. After the global points are chosen, the local search phase begins which points around the chosen point to develop a gradient. The gradient is then used in the neighborhood of the point chosen to estimate a step to take to get closer to an optimal answer. SHC algorithms have been successfully implanted on satellite scheduling; for example, to take advance of its simplicity, computation efficiency [20].

Simulated Annealing (SA) is a process that is similar to SHC with one variation. There is a probability that steps which provide fewer optimum solutions are chosen based on the difference between the objective function at both points. The formula representing if a less-optimum step is chosen is shown below in equation 3 [21]:

$$p = \begin{cases} e^{-\frac{J(\theta_i)-J(\theta_{i+1})}{c}}, J(\theta_i) > J(\theta_{i+1}) \\ 1 \qquad\qquad\qquad\quad , J(\theta_i) \leq J(\theta_{i+1}) \end{cases} \tag{3}$$

Dan Weld accurately outlines a way of visualizing the SA in his CSE 473 slides [22], where it is said that the SA algorithm is similar to allowing to roll a ball down a hill, which by itself would represent HC for minimization of a function. The difference between the two is in SA: the surface is shaking while the ball rolls, which adds randomness into the system as the shaking of the surface is being reduced over time by the cooling factor c. Figure 3 shows an example of how the SA algorithm can outperform SHC and HC algorithms by avoiding the local minimum of the first trough and having the ball make its way down to the global minimum shown by Figure 4 [22].

Figure 3 An example of when SA would outperform HC and SHC by having the probability of avoiding the first local minimum. [22]

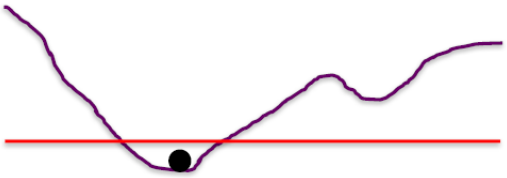

Figure 4 The global optimum solution found by SA. [22]

A Genetic Algorithm (GA) is inspired by the natural evolution (or natural selection) process where high-quality solutions are needed for an optimization problem. It uses lists of answers (or schedules referred to as 'chromosomes') to compare different answers. The GA has four stages, three which loop till completion: initial population, sort, recombination, and mutation. GA is proven to handle functions where the assumptions on the output of the objective functions is not well known. This makes GA an ideal candidate for light curve inversion, as these problems are complex with little knowledge known about the objective function output. On the other hand, the GA algorithm is computationally intensive when compared to other optimization methods. For the implementation of the GA in this paper, the Crossover Operator is defined by a Position-Based Crossover and Mutation Operator by Reciprocal Exchange Mutation.

Particle Swarm Optimisation (PSO) is a relatively recent development in optimization algorithms that was introduced in 1995 [23]. PSO uses a swarm of particles in the solution space that has an associated velocity with them. PSO

moves these points around the solution space when their velocity is affected by how close they are to a local and global maximum. Having the step size being influenced with global and local optimums, the swarm of particles slowly converges on a global solution while still searching local optimum for better global solutions. For more information of PSO, see Poli et al. 2007 [24].

2.3 Light Curve Inversion

As noted earlier, light curve inversion refers to the process of estimating the properties of the object from the light curve. Two main types of light curve inversions are glint analysis and attitude finding. Glint analysis refers to looking at repeated specular reflection off of an RSO, which allows the determination of the spin rate of the RSO. This is done by looking at repeated peaks in a RSO's light curve; this is not always precise as there is the possibility of symmetries causing harmonics of the spin rate to be determined instead of the actual spin rate [25].

Attitude finding gives more information about the RSO, however it normally requires priory information and is more computationally intensive than the spin rate analysis of RSO's [26] [10]. Attitude finding involves estimating the brightness of an RSO and comparing it to the measured brightness of the RSO. The difference between the measured and estimated brightness is used to refine the answer and estimate better attitudes. One further problem that is presented is the brightness produced by the RSO does not directly relate to the attitude of the satellite as multiple attitudes have the possibility of generating the same brightness. To eliminate the redundancy in the possible attitudes, the attitudes are put in a time series which makes it possible to eliminate attitudes with large jumps that were impossible to be performed. To do this, the 1000 best light curve residuals and their corresponding attitude are saved and analysed using the first order derivative analysis; this allows only the possible attitude sequences to be presented. If this is not performed, the 1000 best attitudes will represent 1000^n sequences produced, with n representing the number of images. After the derivative analysis is performed, the attitude sequences are plotted to show all the possible sequences as well as the best possible sequence estimate (shown in Figure 5). While the first derivative analysis performs well, different methods could be used to extract the possible sequences from the 1000 best residuals. Testing different filtering methods was outside of the scope for this paper, however, it is identified and discussed more in the future work section.

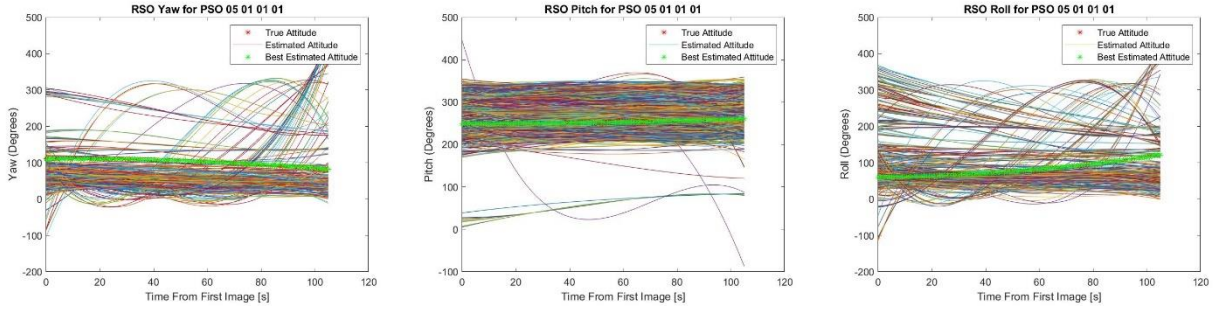

Figure 5 Yaw, Pitch and Roll Possible Sequences, True Sequence, and Best Estimated Attitude

3 Methodology

To perform the comparison of parameterisation algorithms, a simulated environment in MATLAB was used. The Space Based Optical Image Simulator (SBOIS) was used to simulate low resolution images taken from a space-based station. This replicates detections that would be similar to an RSO passing in the FOV of a star tracker camera. In the simulated environment, one sequence was simulated with 20 different attitude profiles for 4 unique satellite shapes to act as the simulated observed data. The unique shapes are shown in Figure 6 to Figure 9, and represent 1U, 3U, Box-wing, and Iridium First Generation satellites. Each parameterisation algorithm ran a maximum of 30 iterations with the convergence rate and final accuracy being used as a figure of merit to compare the performance of the parameterisation algorithm. Table 2 contains the input parameters for each of the parameterisation algorithms:

Table 2 Parameterisation Algorithm Parameter Inputs

Algorithm	Parameter	Value
Gradient Descent	Magnitude to Degrees	30
	Degree Step Max/Min	15/0.1
	Bottom Random Percentage	50%
Stochastic Hill Climbing	Magnitude to Degrees	30
	Degree Step Max/Min	15/0.1
Simulated Annealing	Magnitude to Degrees	30
	Degree Step Max/Min	15/0.1
	Beta	0.99
	Cooling Factor	5
Particle Swarm Optimisation	Max Velocity	30
	Current Velocity Weight	0.9
	Local Optimum Velocity Weight	1.2
	Global Optimum Velocity Weight	1.2
Genetic Algorithm	Cross Over Parameter	0.5
	Mutation Chance	0.01

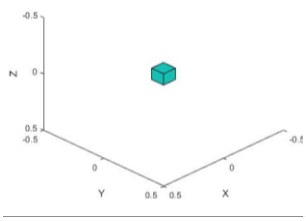

Figure 6 1U Cube Satellite Geometric Model

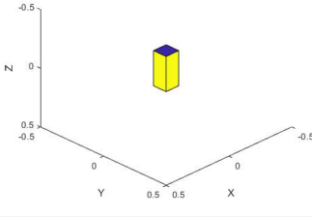

Figure 7 3U Cube Satellite Geometric Model

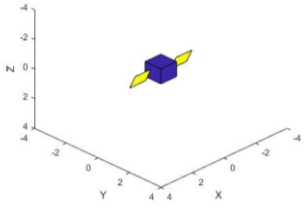

Figure 8 Box-Wing Satellite Geometric Model

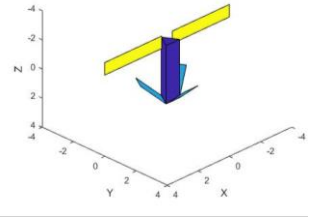

Figure 9 Iridium First Generation Satellite Geometric

4 Results and Discussion

The results for the two figures of merit, accuracy and convergence rate, for each algorithm and each satellite model is shown in Table 3. The average RMSE of the 1000 best iterations for each algorithm is shown in Figure 10 to Figure 12 for each satellite model. The attitude profile residual for 1 of the 20 true sequences is shown for each algorithm and each satellite model in Figure 15 to Figure 16. How each of the 2 figures of merit are calculated is described below.

Two different types of accuracy are looked at in the results: the brightness accuracy and the attitude profile accuracy. The brightness accuracy represents the RMSE of the 1000 best light curve brightness residuals, this given over the iterations of the parameterisation algorithms give insight into the convergence of each. Attitude profile accuracy is the RMSE in the best Yaw, Pitch, and Roll parameters estimated, compared to the true Yaw, Pitch, and Roll parameters for a given sequence. The attitude profile RMSE is then averaged over different true sequences to get an average RMSE for the model and parameterisation algorithm.

The convergence rate is compared both by iteration and computation time, which is calculated from each iteration being timed. The iteration convergence rate is defined as the number of iterations it takes for the Brightness Average RMSE to drop by one half life. The computation convergence rate is the average time it takes to converge one half life.

Table 3 Parameterisation Algorithm Results

Algorithm	Geometric Model	Brightness Average RMSE	Attitude Profile RMSE	Iteration Convergence Rate	Computation Convergence Rate
Gradient Descent	1U	0.0085	4.6	6.8	16.6
	3U	0.0102	4.7	6.7	16.6
	Box Wing	0.0154	5.5	6.8	20.9
	Iridium F.G.	0.0187	5.4	6.9	26.1
Stochastic Hill Climbing	1U	0.0066	12.1	6.3	13.7
	3U	0.0085	11.5	6.3	13.9
	Box Wing	0.0111	10.4	6.2	16.8
	Iridium F.G.	0.0146	10.3	6.5	21.6
Simulated Annealing	1U	0.0062	9.3	6.3	29.1
	3U	0.0081	8.8	6.3	29.0
	Box Wing	0.0103	9.2	6.1	35.0
	Iridium F.G.	0.0137	8.9	6.4	46.9
Particle Swarm Optimisation	1U	0.0035	2.4	5.3	49.6
	3U	0.0049	1.8	5.4	51.0
	Box Wing	0.0056	1.7	5.2	60.1
	Iridium F.G.	0.0080	2.0	5.4	76.2
Genetic Algorithm	1U	0.0074	2.6	6.6	93.8
	3U	0.0093	2.6	6.5	94.1
	Box Wing	0.0126	2.6	6.5	110.6
	Iridium F.G.	0.0171	2.7	6.8	110.0

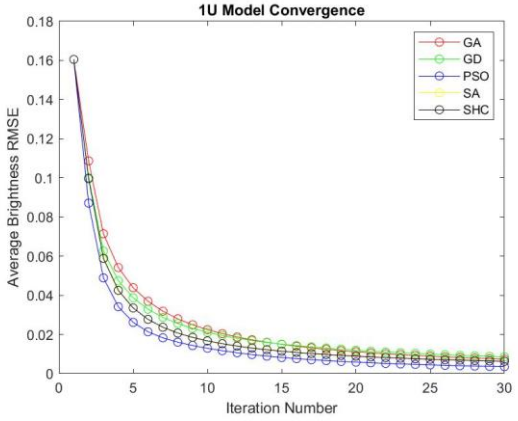

Figure 10 1U Model Algorithm Average RMSE

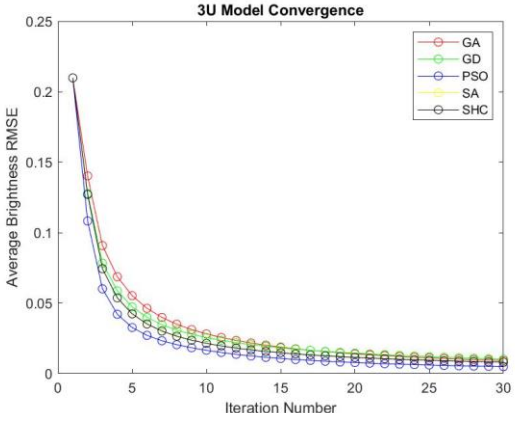

Figure 11 3U Model Algorithm Average RMSE

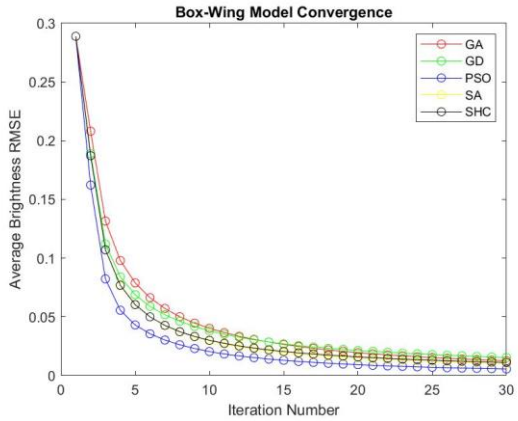

Figure 12 Box Wing Model Algorithm Average RMSE

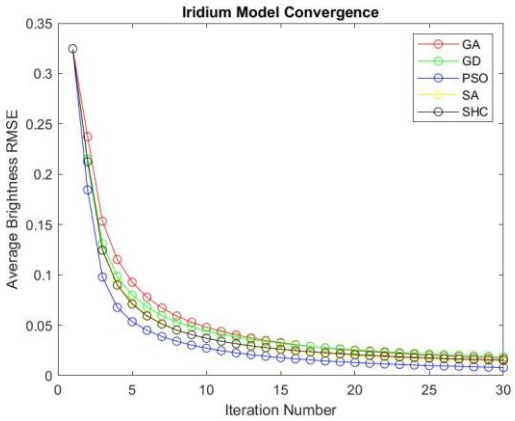

Figure 13 Iridium First Generation Model Algorithm Average RMSE

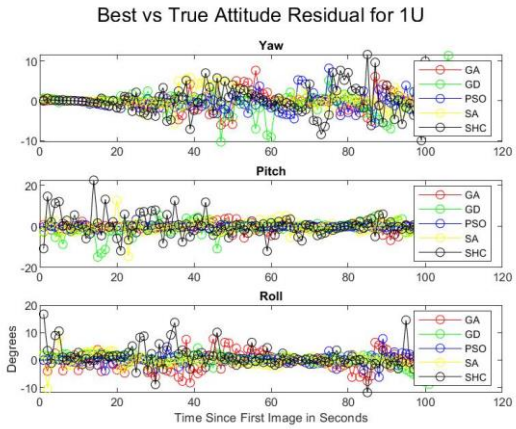

Figure 14 1U Model Attitude Residual

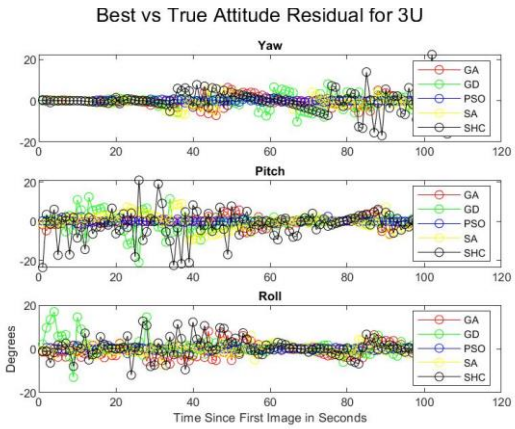

Figure 15 3U Model Attitude Residual

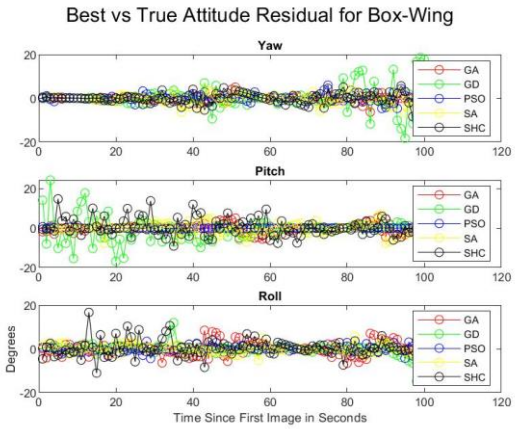

Figure 16 Box Wing Model Attitude Residual

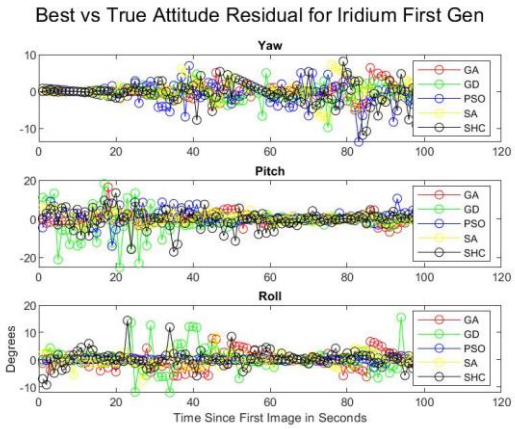

Figure 17 Iridium First Generation Attitude Residual

It can be seen in Table 3 that all the algorithms follow a similar convergence trend, with all algorithms reaching similar average RMSE at 30 iterations. PSO shows the best average RMSE for all models, with SHC and SA having similar average RMSE and performing the second best. This is followed by GA and GD, which performed the worst for

average RMSE. Estimating a RSO's attitude produces a complex design space with many local optimums; GD does not have any way of escaping local optimum, which is hypothesised to contribute to its poor performance. GA has mutations and cross over operations which should allow the algorithm to escape local optimum. The mutation and cross over operation can widely change a child from its original parent; this contributes to a larger solution space being searched with less accurate local optimum evaluation. To allow for better local optimum finding with GA, different intelligent cross over and mutation operators should be tested. Hypothetically, well performing intelligent operators for this solution space would be able to consider the chromosome's relative gene differences, as well as local and global optimum. SA and SHC perform the second best as they both have a random probability of making non-optimal steps to escape the local optimum. In SA, the cooling scheme was used to calculate probability of taking a non-optimal step. A geometric cooling scheme was used, however other cooling schemes such as linear, exponential and logarithmic should be tested and compared. In SHC, the non-optimal step is randomly chosen in this implementation. Implementing more intelligent, non-optimal step probability and direction is likely to improve the performance. It should be noted that implementing intelligent over random methods only improves performance if the intelligent methods accurately represent the solution space. PSO performed very well in contrast to the other algorithms in the solution space; this is attributed in considering a local and global optimum for the updated point calculation. The tuning of the PSO weighting coefficients and velocity calculation should lead to a better convergence for the average RMSE. The brightness average RMSE is a good indication of the performance of the parameterisation algorithms, however the attitude profile RMSE is the value that is looking to be minimized.

It can be seen from the different algorithm attitude profile RMSE that the brightness average RMSE does not fully corelate to the performance when it comes to attitude estimation. SHC and SA were the worst performing algorithms in this category, with SA performing slightly better than SHC. While looking at the top 1000 results for SA and SHC over the iterations, it can be seen that these algorithms estimates are clumped together around the local optimum, not searching the full solution space. To overcome this problem, possible solutions include better tuning of the parameter and the introduction of a tabu list to force solutions away from known local optimum. Tabu lists, commonly used in Tabu search algorithms, force the solution away from previous calculated points to keep searching for a new local and global optimum [27]. In their current implementation, with a performance of approximately 11 and 9 degrees for SHC and SA respectfully, these parameterisation algorithms are not ideal for use for attitude estimation of low-resolution optical detections. It is important to note that a different implementation of SHC and SA in the future could improve the feasibility of these algorithms for attitude estimation of low-resolution optical detections. GD is the next best thing, having an attitude profile RMSE of 4 to 5 degrees depending on the RSO shape model. The current implementation of GD takes the poorest performing attitudes and randomises them to improve the area searched in the solution space. Throughout the various iterations, this causes the 1000 best ones to change and not be as clumped as was seen with SHC and SA. As GD is very likely to get stuck in the local optimum, tabu lists is likely to increase the area searched in solution space, which possibly leads to better attitude optima estimations. GD does not perform the best in attitude profile RMSE but with its quick computation speed; it is feasible for certain implementation of attitude estimation where getting speed is prioritised over accuracy. The best two performing algorithms with similar performance are PSO and GA: PSO performing the best with 1.7 to 2.4 degree RMSE verses GA's 2.6 to 2.7 RMSE across all models. GA, having such a consistent RMSE across all models, is consistent with the cross over operator searching a large solution space but not accurately converge. Implementing more intelligent operators is likely to improve the attitude profile RMSE by allowing better convergence on local optima. PSO's ability to search a complex solution space efficiently considering local and global optima makes it ideal for attitude estimation of low-resolution optical detections. Tuning of GA and PSO will likely lead to more accurate attitude RMSE profile, as well as the addition of higher fidelity local optima searching.

While comparing the different models, it can be seen that there is a similar attitude performance across all models with different algorithms performing differently for each one, GD performs better with the less complex models (such as 1U and 3U) compared to Box-Wing and Iridium First Gen. SHC is reversed where it performs better in the more complex models and worse on the less complex models. PSO and SA perform marginally better in 3U and Box-Wing than in 1U and Iridium First Gen. GA performs approximately the same across all models. While it is not fully known why algorithms perform differently across the models, it hypothesised that the symmetry and complexity of the models are expected to influence the outcome. Having less symmetric RSO should lead to fewer well-performing local optima; though, it would normally increase the complexity of the model in doing that. Increasing the complexity increases the possibility of error to be introduced in the system; this can be seen by the brightness average RMSE increasing as the

model complexity increases. Additionally, more complex models require more computation time, making it a trade-off between accurate modeling and computation speed. More comparison will need to performed on how the model of the RSO's affect the attitude estimate capability of each algorithm.

5 Future Work

There are many areas that require further research in order to get from an academic to a functional framework. The different areas include: testing and tuning more advanced parameterisation algorithms; testing and tuning different filtering methods for the top 1000 attitudes; updating the BRDF models to be more accurate; and performing the analysis in a real verses simulated environment.

By looking at testing more advanced parameterisation algorithms, we can see the implementation of MMEA, unscented Kalman filters, and different machine learning being proven to work for RSO attitude determination. Comparing these methods with PSO and GA will give a better understanding of the algorithms' performance relative to each other, as well as in which situations each algorithm outperforms the other. One example is comparing an uncontrolled (or slow) rotating RSO with a controlled RSO that is performing a slewing maneuver. Identifying which algorithm performs better in each case can also help with the determination between controlled and uncontrolled RSO's. While one implementation of each algorithm was tested in this study, different combinations of these algorithms are also possible; for example, a geometric cooling scheme was used for simulated annealing, regardless of there being many different cooling schemes that could be implemented that would change the algorithm's performance. Currently, the algorithms optimise the attitude for each image separately and then use the derivative information to limit those results. Including the derivative analysis and filtering in the parameterisation algorithms could possibly lead to a better convergence accuracy and rate and is currently being implemented and tested for all the algorithms mentioned in this paper.

Different filtering methods on the Yaw, Pitch and Roll of the best light curve residuals can be implemented to reduce the number of possible attitude sequences and more accurately give the best estimate for attitude. For this paper, a first-order derivative analysis was used to limit the number of possible sequences. This was chosen as it was easy to implement, in the future testing different filtering methods such as; second order derivative analysis, moving window filters, and whether to perform the filtering after the parameterisation algorithm or include it in the parameterisation algorithm. When comparing different types of RSO's, such as controlled verses uncontrolled, the filtering algorithms will also perform differently. While first-order filtering is sufficient for an uncontrolled satellite, it does not handle slewing maneuvers and large spin rate changes effectively and thus requires the implementation of more robust filters. Currently, testing is being performed to see how the different types of filters impact the best estimated sequence, as well as identifying if performing the filtering in the parameterisation algorithm leads to a more efficient convergence rate and accuracy.

The BRDF used for the light curve generation is a significant portion of the objective function. Updating the BRDF to a more accurate or computationally efficient methods will have a significant impact on the results of the optimisation. There are many different known methods for artificial satellite BRDF: the methods outlined in Linares, R. et al. (2014) [14]; Fan, S. & Frueh C. (2019) [28]; and Subbarao, K. & Henderson, L (2019) [29]. Different methods like the Phong model implementation include facet directional reflectance represented by Nu and Nv, which has a possibility of reducing the number of false possible sequences. Different BRDF models have also been shown to represent different RSO shapes and material properties with different accuracy [29] [28]. To properly test different BRDF methods, the accuracy and computation speed should be compared on a range of possible satellite shapes to see which method is the most robust and which method performs best for common RSO shapes. Currently, research is being completed to compare different light curve models against the current defined facet model implementation, such as the methods outlined in [28] [14].

Training and comparing algorithms in a simulated environment are effective ways to demonstrate feasibility, however are useless without the real-world implementations. Moving from a simulated to a real environment is the next big stepping in moving low resolution optical characterisation of RSO's from an academic to an operational idea. One of the biggest challenges in taking this step is having well-labelled detections, from sensor with known parameters, where the target RSO true attitude and shape is known. Currently, thanks to the Defence Research and Development Canada (DRDC), attitude information and ground-based detections of the Radar Constellation Mission (RCM) have been provided to York University to allow for the real-world testing. By using detections of RCM from the Fast Auroral

Imager, as seen in Figure 1, as well as low resolution terrestrial detections, this method feasibility and accuracy will be evaluated for terrestrial and space based observations.

6 Conclusion

In conclusion, this paper demonstrates the feasibility of using different parameterisation algorithms for light curve inversion in a simulated environment. While all algorithms showed the ability to converge to different attitude sequences, PSO and GA showed the best results for attitude residual accuracy with both having under 3 degrees RMSE for all models. SHC and SA provided a good convergence rate but will need to be tuned to search a larger solution space.

Another finding from this paper was the different areas that still needs improvement to move from academic to operational model. Below is a summary of the areas identified to enable operational model of low-resolution optical characterisation:

- Implementation on real world data
- Improving filtering methods to handle both controlled and uncontrolled RSO's
- Tuning of individual parameterisation algorithm and implementation of meta-heuristics
- Characterise BRDF models performance with different RSO shapes and detection angles
- Generation of standard data sets with known parameters for algorithm performance testing
- Determination of minimum detection statistics required for accurate attitude estimation

7 References

[1] D. Burandt, D. Hampf, J. Rodmann and W. Riede, "INTERPRETATION OF LIGHT CURVES BASED ON SIMULATION SOFTWARE," in *International Astronautical Congress (IAC)*, Adelaide, 2017.

[2] C. R. Singletary and F. K. Chen, "Simulating Complex Satellites and a Space-Based Surceillance Sensor Simulation," in *AMOSTech* , 2007.

[3] M. R. Ackermann, R. R. Kiziah, P. C. Zimmer, J. T. McGraw and D. D. Cox, "A SYSTEMATIC EXAMINATION OF GROUND-BASED AND SPACE-BASED APPROACHES TO OPTICAL DETECTION AND TRACKING OF SATELLITES," in *31st Space Symposium*, 2015.

[4] B. Lal , A. Balakrishnan, B. M. Caldwell, R. S. Buenconsejo and S. A. Carioscia, "Global Trands in Space Situational Awareness (SSA) and Space Traffic Management," IDA SCIENCE & TECHNOLOGY POLICY INSTITUTE, 2018.

[5] B. Wallace , R. Scott and A. Spaans, "The DRDC Ottawa Space Surveillance Observatory," in *AMOSTech* , 2007.

[6] L. Scott, S. Thorsteinson, D. Bedard, B. Cotten and R. E. Zee, "Canadian Ground Based Optical Observations of the CANX-7 Sail Deployment," in *CASI/ASTRO*, 2018.

[7] L. Scott, B. Wallace, M. Sale, M. Levesque and S. Thorsteinson, "Toward Microsatellite Based Space Situational Awareness," in *The Advanced Maui Optical and Space Surveillance Technologies Conference* , 2013.

[8] S. Clemens, R. Lee, P. Harrison and W. Soh, "Feasibility of Using Commercial Star Trackers for On-Orbit Resident Space Object Detection," in *AMOS Tech* , 2019.

[9] University of Calgary , "e-POP data set website," [Online]. Available: https://epop-data.phys.ucalgary.ca/.

[10] J. R. Snell, "Optimizing orbital debris monitoring with optical telescopes," in *2010 Advanced Maui Optical and Space Surveillance Technologies Conference*, 2010.

[11] G. A. McCue, J. G. Williams and J. M. Morford, "Optical Characteristics of Artificial Satellites," *Planet. Space Sci,* vol. 19, pp. 851-868, 1971 .

[12] W. E. Krag, "Visible Magnitude of Typical Satellites in Synchronous Orbits," 1974.

[13] M. D. Hejduk, "Specular and Diffuse Components in Spherical Satellite Photometric Modeling," in *The Advanced Maui Optical and Space Surveillance Technologies (AMOS) Conference*, 2011.

[14] R. Linares, M. K. Jah, J. L. Crassidis and C. K. Nebelecky, "Space Object Shape Characterization and Tracking Using Light Curve and Angles Data," *Journal of Guidance Control and Dynamics,* 2014.

[15] M. Kaasalainen, "Optimization Methods for Asteriod Lightvurve Inversion I. Shape Determination," *Icarus,* vol. 153, pp. 24-36, 2001 .

[16] M. Kaasalainen, "Optimization Methods for Asteriod Lightcurve Inversion II. The Complete Inverse Problem," *Icarus,* vol. 153, pp. 37-51, 2001.

[17] K. Subbarao and L. Henderson, "Observability and sensitivity analysis of lightcurve measurement models for use in space situational awareness," *Inverse Problems in Science and Engineering,,* pp. 1399-1424, 2019.

[18] M. Howard, B. Klem and J. Gorman, "RSO Characterization with Photometric Data Using Machine Learning," 2015.

[19] S. Ruder, "An overview of gradient descent optimization algorithms*," 2016.

[20] S. Baluja, "An Empirical Comparison of Seven Iterative and Evolutionary Heuristics for Static Function Optimization," in *Eleventh International Conference on Systems Engineering* , 1996.

[21] A. Corana, M. Marchesi, C. Martini and S. Ridella, "Minimizing Multimodal Functions of Continous Variables with the "Simulated Annealing" Algorithm," *ACM Transactions on Mathmatical Software* , 1987.

[22] D. Weld, "CSE 473: Artificial Intelligence Power Point," 2016.

[23] J. Kennedy and R. Eberhart, "Particle Swarm Optimization," in *IEEE International Conference on Neural Networks* , 1995.

[24] R. Poli, J. Kennedy and T. Blackwell, "Particle swarm optimization," *Springer Science,* 2007 .

[25] N. Koshkin, S. Strakhova and S. Leonid, "Remote Sensing of the EnviSat and Cbers-2B satellites rotation around the centre of mass by photomerty," 2016.

[26] B. K. Bradley and P. Axelrad, "Lightcurve Inversion For Shape Estimation of GEO Objects from Space-Based Sensors," 2014.

[27] W.-C. Lin and D.-Y. Liao, "A Tabu Search Algorithm for Satellite Image Scheduling," in *2004 IEEE International Conference on Systems, Man and Cybernetics*, 2004.

[28] S. Fan and C. Frueh, "A Direct Light Curve Inversion Scheme in the Presents of Measurement Noise," *The Journal of the Astronautical Sciences,* 2019.

[29] K. Subbarao and L. Henderson, "Obervability and sensitivity analysis of lightcurve measurement models for use in space situational awareness," *Inverse Problems in Science and Engineering* , 2019.

[30] P. W. Kervin, D. Hall, M. Bolden and J. Toth, "Phase Angle: What is it Good For?," 2020.